

A NOVEL APPROACH FOR THE FABRICATION AND ANALYSIS OF 3D PRINTING FILAMENT MATERIALS

¹ POTNURU SUMANTH, ² MATTA PRADEEP, ³ PAPPU PAVAN KUMAR, ⁴ MUDILI DILLESWARI, ⁵ KOMARAM YUVARAJU, ⁶ KONDETI VEDHAGAYATRI, ^{7,*} Dr. M. SRINIVASA RAO

^{1,2,3,4,5,6,7}Department of Mechanical Engineering, GMR Institute of Technology, Rajam-532127, India

Emails: srinivas.m@gmrit.edu.in, potnurusumanth389@gmail.com, mattapradeep4@gmail.com, pavankumar082005@gmail.com, mudilidilleswari@gmail.com, komaramyuvaraj@gmail.com, vedhagayatri48@gmail.com

*Corresponding author: Dr.M. Srinivasa Rao. Contact number: 9000542349

Email: srinivas.m@gmrit.edu.in

DOI: 10.63001/tbs.2025.v20.i03.S.I(3).pp1487-1504

KEYWORDS:

FDM, Additive Manufacturing, 3D Printing, Polymer, Hybrid Composite Filaments, Infill Pattern Geometry, Mechanical Properties, PLA, ABS, Nylon, PETG, PLA-Copper, PLA-Bronze, Infill Density, Tensile, Compressive, Impact, Shear Tests, Structural Performance, Statistical Analysis.

Received on:

06-09-2025

Accepted on:

02-10-2025

Published on:

11-11-2025

ABSTRACT

AM technologies have rapidly evolved, and the most popular method for polymer-based 3D printing applications is FDM. The ability to tailor mechanical properties through both material selection and, importantly, process settings such as infill geometry has created new opportunities for sophisticated engineering applications. This research paper aims to investigate the effect of changes in the internal infill pattern geometry on the mechanical properties of normal and hybrid composite filaments fabricated through FDM. The presented study makes use of four normal materials, namely (PLA) Polylactic Acid, (ABS) Acrylonitrile Butadiene Styrene, Nylon, (PETG) Polyethylene Terephthalate Glycol and two different commercially available hybrid material combinations, namely PLA-Copper and PLA-Bronze. For all materials, samples were fabricated with a fixed 60% infill density while the internal infill pattern geometry was systematically varied. Standardized mechanical tests were performed to determine performance attributes and structural integrity for each material-pattern combination. The testing included tensile, compressive, impact, and shear tests. A statistical analysis was done on the resulting experimental data. Thereafter, this work offers an essential and new understanding of how the infill pattern influences the structural performance for certain hybrid materials used in high-performance additive manufacturing applications and thus provides recommendations for refined design strategies.

1.INTRODUCTION

3D printing, also referred to as additive manufacturing (AM), has become a game-changing technology for high-precision and environmentally friendly production. Because of its affordability, adaptability in design, and compatibility with a wide variety of thermoplastic polymers, Fused Deposition Modeling (FDM) is the

most used AM technology. By extruding semi-molten filament through a heated nozzle, the FDM technique builds parts layer by layer, facilitating quick prototyping and the creation of bespoke products for the engineering, biomedical, aerospace, and automotive industries. Recent advancements in FDM research emphasize three primary directions-environmental sustainability, process parameter optimization, and material Innovation, Sustainable development goals have encouraged the use of biodegradable and renewable polymers, such as Polylactic Acid (PLA), which minimize carbon footprint while maintaining acceptable mechanical performance. At the same time, traditional materials such as Acrylonitrile Butadiene Styrene (ABS), Polyethylene Terephthalate Glycol (PETG), and Nylon (PA) continue to dominate functional prototyping because of their superior strength, toughness, and thermal stability. Furthermore, the integration of composite and hybrid filaments, Including metal-filled PLA.

1.1 POLYLACTIC ACID (PLA)

One of the most widely utilized biodegradable polymers in fused deposition modeling (FDM) is polylactic acid (PLA). It is an eco-friendly substitute for plastics made from petroleum because it is made from renewable agricultural resources like corn starch, sugarcane, or cassava. Because of its exceptional surface smoothness, great dimensional precision, and low warping, PLA is a good choice for both aesthetic and prototype purposes. Because of its comparatively low melting temperature (between 180 and 220°C), printing can be done with less thermal distortion and less energy.



Fig 1: PLA Material

PLA's usage in functional or load-bearing applications is, however, limited by its brittleness, low impact resistance, and limited heat stability. Researchers have created PLA composites reinforced with fibres, nanoparticles, or metal powders to improve strength, toughness, and thermal performance in order to get around these limitations.

1.2 BUTADIENE ACRYLONITRILE STYRENE (ABS)

A petroleum-based thermoplastic with a reputation for toughness, impact resistance, and heat resistance is Acrylonitrile Butadiene Styrene (ABS). It is extensively utilized in consumer goods, automotive applications, and engineering components. Unlike PLA, ABS can tolerate higher service temperatures and provides strong inter-layer adhesion in FDM printing.

Notwithstanding these benefits, ABS has drawbacks, including a high propensity for warping and the release of volatile organic compounds (VOCs) during printing. For dimensional accuracy and user safety, a heated bed and regulated environment are necessary. It is appropriate for structural components and functional prototypes due of its exceptional mechanical resilience. Researchers have looked into ABS blends with PLA or carbon fibers to further enhance performance, combining strength with better printability and less environmental effect.



Fig 2: ABS Material

1.3 GLYCOL OF POLYETHYLENE TEREPHTHALATE (PETG)

An amorphous copolyester called Polyethylene Terephthalate Glycol (PETG) fills the gap between PLA and ABS by providing a combination of strength, flexibility, and printing ease. PETG minimizes warping and is appropriate for transparent or functional components because of its low shrinkage, strong chemical resistance, and better layer adhesion. It can create items with excellent clarity and durability and has a moderate printing temperature range of 220 to 250°C.

PETG is completely recyclable and supports sustainable production methods, although it is not biodegradable like PLA. Because of its sensitivity to moisture, it is advised to dry the filament before using it. PETG is frequently chosen for use in biological models, protective casings, and mechanical components because of its robust inter-layer bonding and longevity.



Fig 3: PETG Material

1.4 NYLON (PA, OR POLYAMIDE)

The semi-crystalline engineering polymer nylon (PA) is renowned for its exceptional fatigue strength, wear resistance, and toughness. It is extensively utilized in industrial and mechanical applications where durability and flexibility are required. Gears, hinges, and working prototypes can all benefit from nylon's exceptional impact strength and elongation at break in FDM.

However, nylon's strong moisture absorption and propensity to warp might make printing more difficult, requiring filament pre-drying and controlled climatic conditions.

Fig 4:

Nylon Material

Variants of nylon reinforced with carbon fiber or glass fiber are currently being utilized to increase stiffness and dimensional stability due to developments in composite formulations. Nylon's importance in cutting-edge engineering and performance-critical 3D printing applications has grown as a result of these advancements.

1.5 PLA+ BRONZE COMPOSITE

PLA and finely ground bronze particles are combined to generate the PLA + Bronze composite, a hybrid filament. This combination gives the printed component a metallic sheen and better wear resistance by increasing its density, stiffness, and visual attractiveness. When compared to pure PLA, the bronze particles improve surface stiffness and hardness by acting as micro-reinforcements. Because bronze has a high heat conductivity, it also exhibits better heat dissipation during printing, which results in smoother surfaces and less distortion.

PLA + Bronze composites, which combine biodegradability with a metallic look and tactile feel, are frequently utilized in prototypes, artistic creations, and decorative products.



Fig 5: PLA Bronze Material

1.6 PLA + COPPER COMPOSITE

The PLA + Copper combination creates a filament with improved density, mechanical strength, and thermal conductivity by integrating copper powder into a PLA matrix. Copper particles provide the printed product a noticeable metallic sheen while also increasing its rigidity and durability.

This combination is also appropriate for biomedical and hygienic applications due to copper's inherent antibacterial qualities. The composite retains its good printability and adhesion properties despite the modest increase in filament weight caused by the higher density. Thus, PLA + Copper offers a sustainable route to 3D-printed parts that are performance-focused, visually pleasing, and useful.



Fig 6: PLA + Copper Material

2. LITERATURE REVIEW

Fused Deposition Modelling (FDM), a key method in additive manufacturing (AM), is used to produce complicated, lightweight components with great material efficiency. FDM is widely used for both industrial and research applications because it provides substantial benefits in terms of cost, usability, and customization. The mechanical, thermal, and environmental performance of polymers like polylactic acid (PLA), nylon, polyethylene terephthalate glycol (PETG), and acrylonitrile butadiene styrene (ABS) has been the subject of numerous studies. These studies have focused on the effects of process parameters, such as layer thickness, infill density, raster orientation, and speed, on strength, stiffness, and dimensional accuracy. Recent research trends have shifted toward improving the sustainability and functionality of printed components through the use of composite and hybrid filaments.

It has been demonstrated that adding reinforcing materials like copper, bronze, glass fiber, and carbon fiber to polymer matrices like PLA and PETG improves their tensile strength, flexural characteristics, and thermal stability. Because they combine a metallic look, increased rigidity, and superior surface polish with PLA's biodegradability and printability, metal-filled PLA composites such as PLA–Copper and PLA Bronze have attracted special interest. However, issues including lower ductility, increased brittleness, and nozzle wear are still being researched. Here are some referred papers with the author and the year of publish.

Alarifi et al.(2023) investigated FDM-printed PETG reinforced with 20% carbon fibers across solid, circular, hexagonal auxetic, and re-entrant designs. Tensile, flexural, and compressive tests ASTM (D3039, D790, D695) on Carbon PETG showed optimized strength at 0.25 mm layer thickness and 20% infill. FEA validated experiments, and SEM revealed fracture morphology. Results confirmed significant mechanical improvements and auxetic behaviour variations without altering chemical composition.

Shanmugam et al.(2024) reviewed thermal behaviour of neat polymers and fiber-filled composites (glass, carbon, natural, and filled) in FDM printing. Key parameters—nozzle temperature, layer height, and speed—were identified for thermal optimization. Glass and carbon fiber composites enhanced conductivity and stability, while fillers BN, graphene) further improved performance. Annealing and filler alignment emerged as effective strategies for crystalline structure enhancement.

Liu et al.(2025) employed WOA-enhanced SVR and NSGAIII multi-objective optimization to balance dimensional accuracy and print time in FDM. Enhanced Latin Hypercube Sampling (50 runs) provided data for predictive modelling RMSE 0.0439. Optimized parameters (speed, layer thickness, temperatures) achieved 3%

error in experiments. A prosthetic case study (40.80 19.92 16.70 mm) demonstrated 98% dimensional conformity, validating the machine-learning approach.

Gonzalez et al.(2023) evaluated the effects of graphene nanoplatelet and carbon nanotube additions 0.52% on mechanical strength, thermal stability, and electrical conductivity of PLA filaments. Tensile and flexural tests revealed up to 20% improvements in modulus at 1% loading. DSC and TGA analyses showed enhanced crystallization behaviour and a 15°C increase in decomposition temperature. Electrical conductivity reached 10^{-3} S/m, enabling potential sensing applications. Optimal dispersion was achieved using twin screw extrusion and sonication.

Wang et al.(2023) developed a dual extrusion FDM process to co print PLA insulating matrix and conductive silver nanoparticle infused thermoplastic ink. Electrical line widths of 200 μ m were achieved with 0.5 Ω /cm resistivity. Process optimization included nozzle temperatures 210 °C for PLA, 190 °C for ink and interlayer cooling. Mechanical flexibility tests showed 10^4 bending cycles without conductivity loss. The approach enabled rapid prototyping of embedded circuits and strain sensors.

Chen et al.(2025) investigated the low cycle fatigue performance of ABS and ABS CF composites under tension–tension loading. SN curves for neat ABS showed fatigue life of 10^5 cycles at 60% UTS, while ABS CF 15% exhibited a twofold increase. Fractography revealed crack initiation at interlayer interfaces. Raster angle (0° vs. 45°) significantly influenced fatigue life, with 0° orientation achieving 30% longer life. The authors proposed a modified Paris law to predict crack growth in FDM parts.

Moreno et al.(2024) conducted a cradle to gate LCA of filaments produced from post consumer PET bottles. Using Sima Pro and Recipe method, they compared virgin PETG and recycled PETG, finding a 30% reduction in global warming potential and 25% reduction in energy consumption for recycled materials. Mechanical testing confirmed comparable tensile strength 45 MPa and modulus. The study identified sorting efficiency and washing processes as key impact drivers.

Kim et al.(2022) explored carbon fiber reinforced PEEK composites printed via high temperature FDM. Fiber contents of 20-40% increased tensile strength to 180 MPa and storage modulus by 50% at 25 °C. Dynamic mechanical analysis showed glass transition shifts from 143 °C to 150 °C. Thermal cycling (50 °C to 120 °C) exhibited 2% dimensional change. The composites met aerospace grade requirements for structural components.

Rahman et al.(2020) designed and evaluated two novel PLA scaffold geometries HDFCPS and RDAPS) alongside three conventional designs using FDM and PLA material. Finite element analysis and experimental compression tests (ASTM D695) assessed stress distribution, deformation, porosity 80%, surface

area, and weight. TOPSIS multi-criteria decision analysis (max stress, deformation, surface area, weight) ranked HDFCPS highest, with 35.3% greater load-bearing capacity than RDAPS. Results emphasized improved mechanical compatibility and potential for vascularization in bone tissue engineering.

Kamaal et al.(2020) investigated the effects of build direction, infill percentage, and layer height on tensile and impact strength of chopped carbon fiber-reinforced PLA composites 5.5% using FDM. Tensile (ASTM D638) and Izod impact (ASTM D256) tests revealed that 0° building direction, 80% infill, and 0.2 mm layer height maximized strength. TOPSIS optimization identified the optimal parameter set for high strength with minimal material. The study highlighted critical parameter interactions and provided guidelines for CFPLA part fabrication.

Fracture Behavior of 3DPrinted Fiber-Reinforced Nylon Khosravani and Reinicke examined how fiberglass reinforcement volume 520 vol% influences fracture resistance of FFF-printed nylon specimens. Coupons were designed in STL, printed layer-by-layer, and subjected to uniaxial tensile tests to record fracture loads and stress–strain curves. Increased fiber content doubled tensile strength and enhanced fracture energy compared to unreinforced nylon. Microstructural analysis revealed fiber pull-out and matrix cracking mechanisms, offering guidelines for designing 3D-printed fiber-reinforced composites with superior fracture toughness.

Mudakavi et al.(2022) Performed a comprehensive DOE on PLA and PLA composites Al, Cu, CF, Brass; 25 vol% printed by material extrusion to quantify tensile UTS/modulus and flexural strength versus layer height, print angle, and speed, supported by FESEM fracture analysis and analytical strength models. Carbon fiber and brass gave the largest modulus gains; composites outperformed neat PLA in flexural tests more than in tensile. Fracture modes were predominantly intra-laminar, with CF promoting trans-laminar failure 4 due to higher aspect ratio. Optimization indicated print angle as the dominant factor affecting strength responses.

Bakhtiari et al.(2024) Investigated how extrusion width, layer height, print speed, and nozzle temperature affect quasi-static compression and compressive fatigue of 60% porosity gyroid PLA scaffolds made via FFF using a Taguchi design and thermography. Extrusion width governed static properties, with 0.65 mm yielding compressive strength 67 MPa, plateau stress 89 MPa, and modulus 200215 MPa. Fatigue resistance was maximized at low nozzle temperature 190 °C; scaffold temperature rose to 39 °C but remained below T_g, so structural integrity was unaffected. CT confirmed 5860% porosity and 750780µm interconnected pores aligned with design.

San Andrés et al.(2023) characterized raw filament and 3D-printed PLA and ABS under accelerated UV and thermal ageing to assess their long-term behaviour for fine art. Both filaments and printed samples exhibited chemical, morphological, and colorimetric changes: ABS showed significant property degradation after UV and heat, including surface cracking and colour shifts, while PLA experienced minimal UV effects but notable thermal aging-induced embrittlement. No form dependent differences were observed. Results inform conservation strategies for 3D-printed artworks

Pozorski & Andrzejewski. identified orthotropic elastic properties of FFF PLA via tensile, bending, and Iosipescu shear tests, comparing extensometer, strain gauges, and DIC measurements. DIC and extensometer agreed on Young's modulus 3.5GPa, while strain gauges overestimated 4.2GPa. Shear tests revealed complex failure modes due to anisotropy from deposited strips. The work validated DIC as reliable and provided a full set of elastic constants for accurate orthotropic modelling of printed PLA structures.

Mishra et al.(2025) Aimed to quantify how layer thickness 0.1-0.3 mm, infill density 50-90%, and printing speed 30-50 mm/min affect the compressive behaviour of PLA ceramic composite parts made by FDM for biocompatible, load-bearing uses. Conducted compression testing to extract σ_y , σ_{max} , and σ_p , and used SEM/EDX to study voids, interlayer bonding, and particle distribution. Found that decreasing layer thickness and speed while increasing infill density raised σ_y from 4.3 \rightarrow 9.5 MPa, from 0.4 \rightarrow 0.8 GPa, σ_{max} from 15 \rightarrow 39 MPa, and σ_p from 26 \rightarrow 58 MPa due to better bonding and reduced hatch spacing. Identified micro-voids and coarse layers as main failure initiators at high thickness and low density, guiding parameter windows for tougher bio-composites.

3. METHODOLOGY

3.1 SELECTION AND PREPARATION OF MATERIALS

This study focuses on analyzing the mechanical performance of normal filements and specialized hybrid composite filaments suitable for FDM. All these materials allow for the study of how infill geometry interacts with unique material matrices.

Materials Utilized:

- PLA : Polylactic Acid.
- ABS : Acrylonitrile Butadiene Styrene.
- PETG : Polyethylene Terephthalate Glycol
- Nylon

- PLA-Copper Composite: A Polylactic Acid (PLA) matrix infused with fine copper powder.
- PLA-Bronze Composite: A Polylactic Acid (PLA) matrix infused with fine bronze powder.

All materials were handled and stored according to manufacturer recommendations to prevent moisture absorption, which could compromise print quality and mechanical integrity.

3.2 TEST SPECIMEN DESIGN, MODELING, AND INFILL PATTERNS

All test specimens were designed using CATIA software to ensure dimensional accuracy and precise internal geometry control, then exported in the Standard Tessellation Language (STL) format.

To ensure the experimental results are comparable and validate the structural integrity of the components, all specimens were designed in strict compliance with relevant ASTM International standards.

These are the designed specimens in CATIA

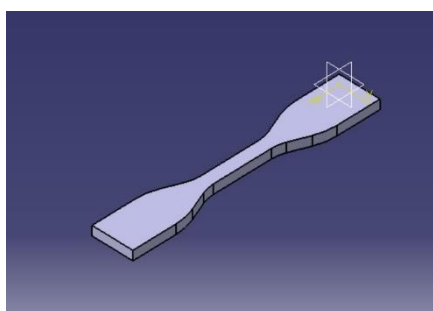


Fig 7.1: Tensile test specimen

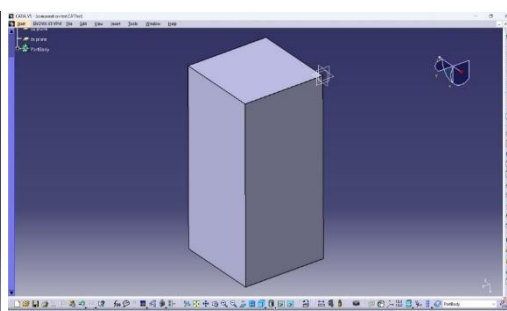


Fig 7.2: Compression test specimen

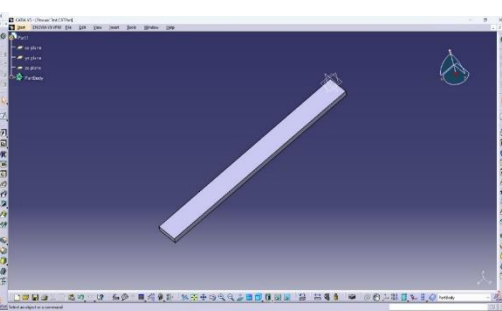


Fig 7.3: Flexural test specimen

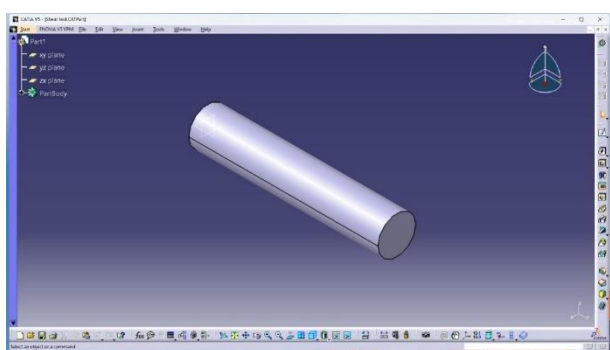


Fig 7.4: Shear test specimen

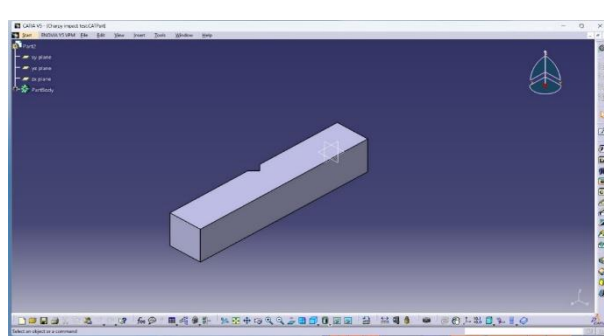


Fig 7.5: Impact test specimen

The primary experimental variable was the internal infill pattern geometry. Specimens were designed and sliced to incorporate the following four geometries:

Grid, Triangular, Concentric and Zig-zag

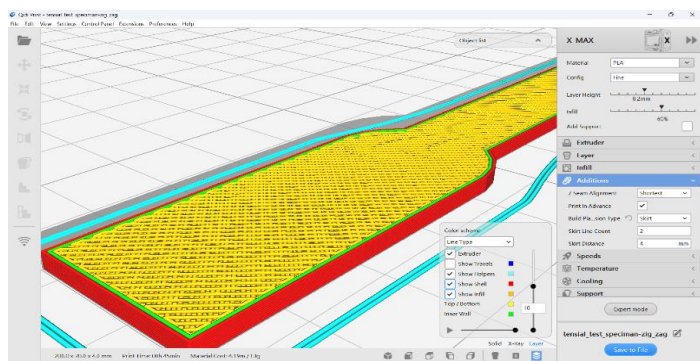


Fig 8.1: Zig-zag pattern

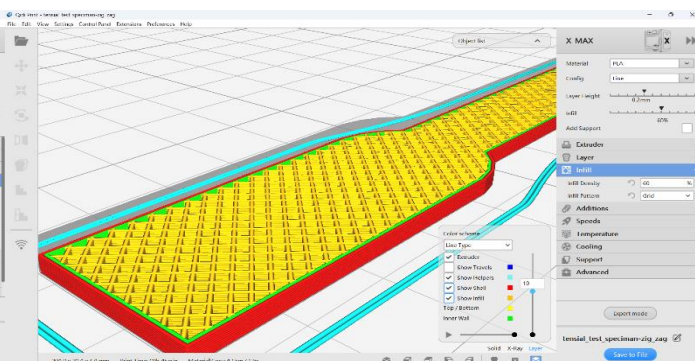


Fig 8.2: Triangular pattern

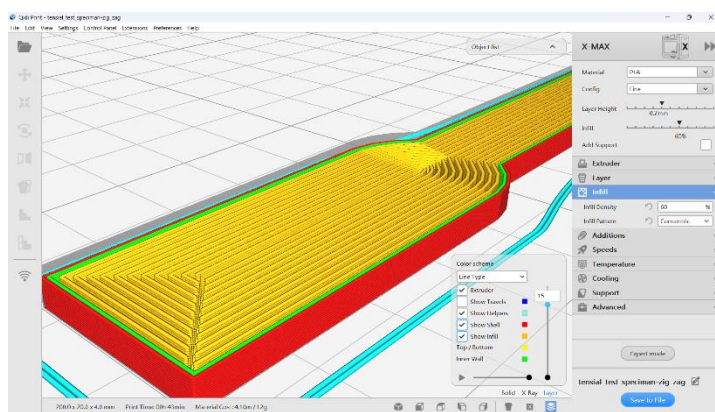


Fig 8.3: Concentric pattern

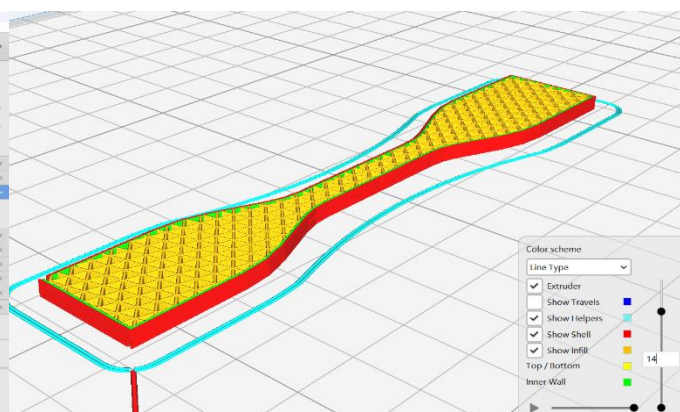


Fig 8.4: Grid pattern

3.3 3D PRINTING PARAMETERS AND SAMPLE PREPARATION

Samples were fabricated using a standard Fused Deposition Modeling (FDM) 3D printer. To isolate the effect of the infill pattern, all other printing parameters were held constant and uniform across all materials and patterns.

Parameter	Value
Nozzle Temperature	210°C
Bed Temperature	60°C
Layer Height	0.2 mm
Infill Density	60%
Print Speed	50 mm/s
Nozzle Diameter	0.4 mm

The prepared samples are

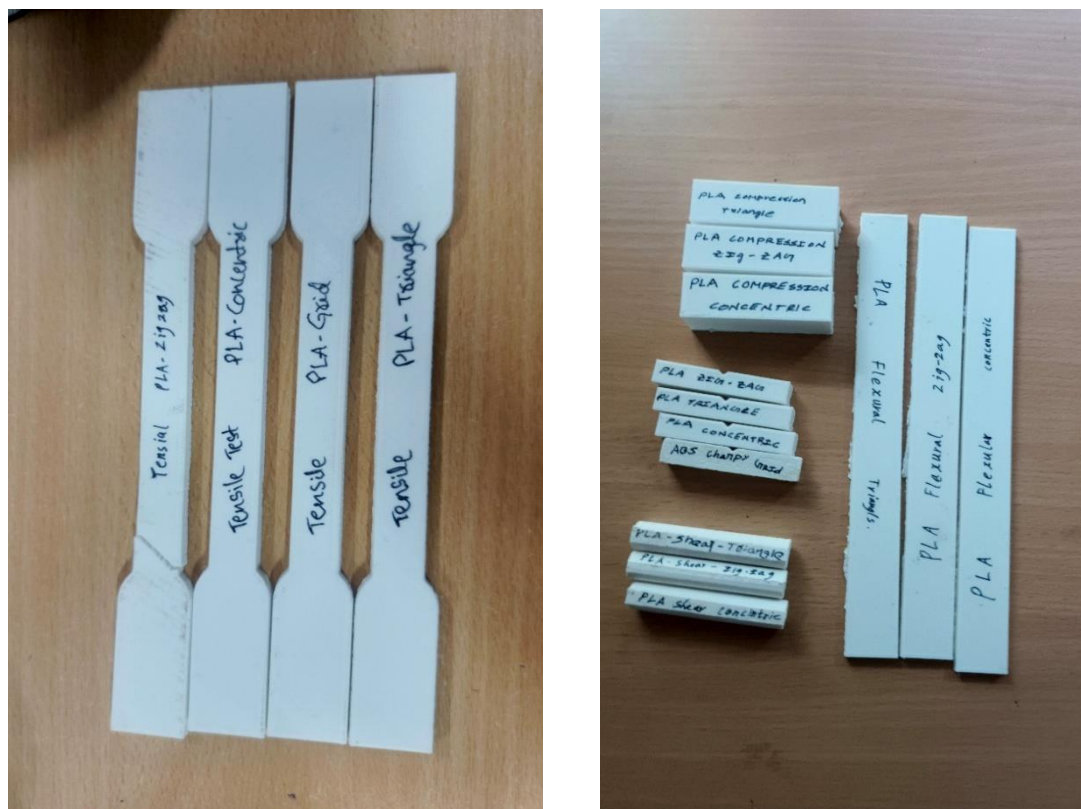


Fig 9,10: All printed materials for the different tests with the infill patterns

3.4 MECHANICAL TESTING PROCEDURES

The structural integrity and mechanical performance of the printed specimens were systematically evaluated using five distinct mechanical tests. All tests were conducted on calibrated electromechanical testing equipment in a controlled environment.

Test	Objective	Output Data
Tensile Testing	To determine the material's response to uniaxial pulling force.	Ultimate Tensile Strength, Elastic Modulus, Elongation at Break.
Compression Testing	To determine the material's resistance to crushing force.	Compressive Strength, Compressive Modulus.
Impact Testing	To measure the material's energy absorption capability (toughness) under sudden loading.	Impact Energy (Joules/m).

Shear Testing	To determine the material's resistance to forces parallel to the material cross-section.	Shear Strength.
Flexural Testing	To measure the material's behavior under bending stress (3-point or 4-point bending).	Flexural Strength, Flexural Modulus.

After testing the deformed shapes of the printed specimens are

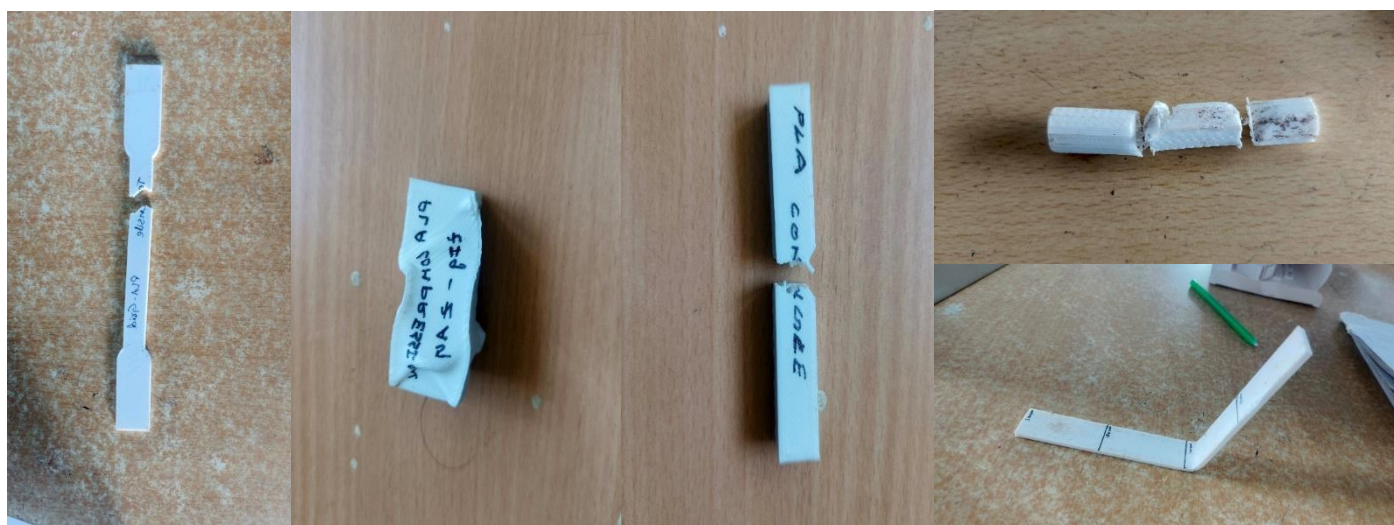


Fig 11: The deformed shapes of tensile, compression, impact, shear and flexural test specimens after testing

3.5 DATA COLLECTION AND STATISTICAL ANALYSIS

Following mechanical testing, all raw data (e.g., force-displacement curves, energy values) was collected, tabulated, and processed.

A statistical analysis was performed using methods such as Analysis of Variance (ANOVA) to determine if the differences observed between the mechanical properties of the four infill pattern groups are statistically significant. Furthermore, the mean and standard deviation for each group were calculated to assess the reliability and consistency of the printed parts.

The experimental results will be compared against established literature values and theoretical ranges for PLA-based composites to provide context and validate the findings.

3.6 INTERPRETATION OF RESULTS AND FORMULATION OF RECOMMENDATIONS

This final stage of the methodology involves interpreting the statistically analyzed data to achieve the research goal. The key effects of the Grid, Triangular, Concentric, and Zig-zag infill patterns on the durability, strength, and toughness of the PLA-Copper and PLA-Bronze hybrid materials will be examined. The study will identify

the optimal infill geometry for high-performance applications and conclude by suggesting refined guidelines for the choice of infill patterns in FDM applications requiring improved mechanical qualities.

This structure now provides a clear, defensible path from material selection to final recommendation.

My main suggestion for you is to fill in the exact values (highlighted in the table in section 3.3) used for your printing parameters, as these are mandatory for a reproducible methodology. Let me know if you'd like me to elaborate on the setup for any of the specific mechanical tests!

4.RESULTS & DISCUSSIONS

4.1 MECHANICAL PERFORMANCE OF PLA BY INFILL PATTERN

The structural integrity of Polylactic Acid (PLA) specimens was evaluated across four infill patterns—Grid, Concentric, Triangles, and Zig-zag—at a fixed 60% density. The results show that the internal geometry significantly dictates the optimal mechanical property.

PLA (Polylactic Acid)

Pattern	Tensile (MPa)	Compression (MPa)	Flexural (MPa)	Shear (MPa)	Impact Charpy (J)
Grid	35	62.5	57.5	22.5	2.5
Concentric	40	57.5	52.5	26.5	3
Triangles	38	67.5	62.5	24.5	2.5
Zig-zag	37	62.5	57.5	23.5	2.5

Fig 12.1:The obtained values from the tests



Fig 12.2:Graph for the Tensile test values

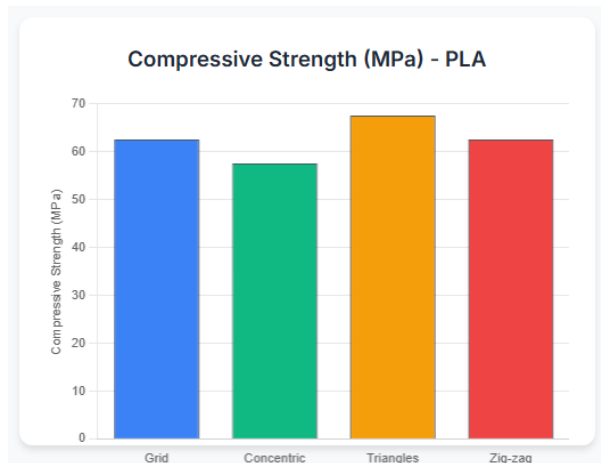


Fig 12.3:Graph for the Compression test values



Fig 12.4:Graph for the Shear test values

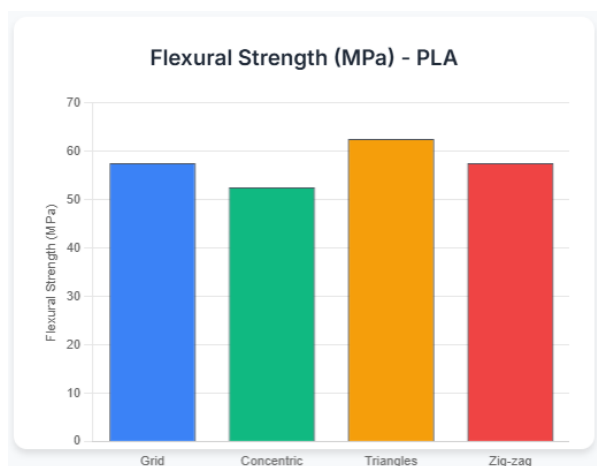


Fig 12.5:Graph for the Flexural test values

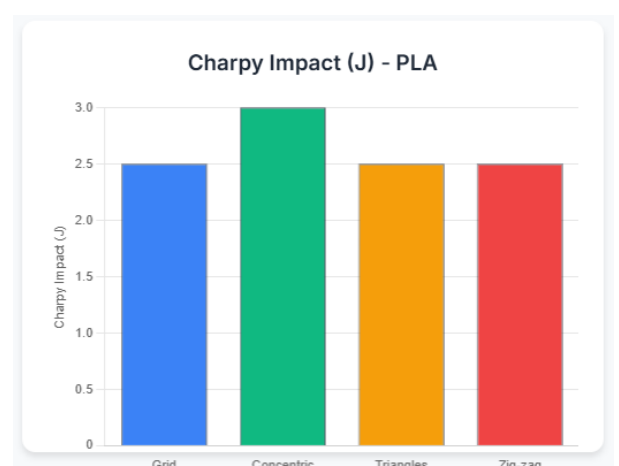


Fig 12.6:Graph for the Impact test values

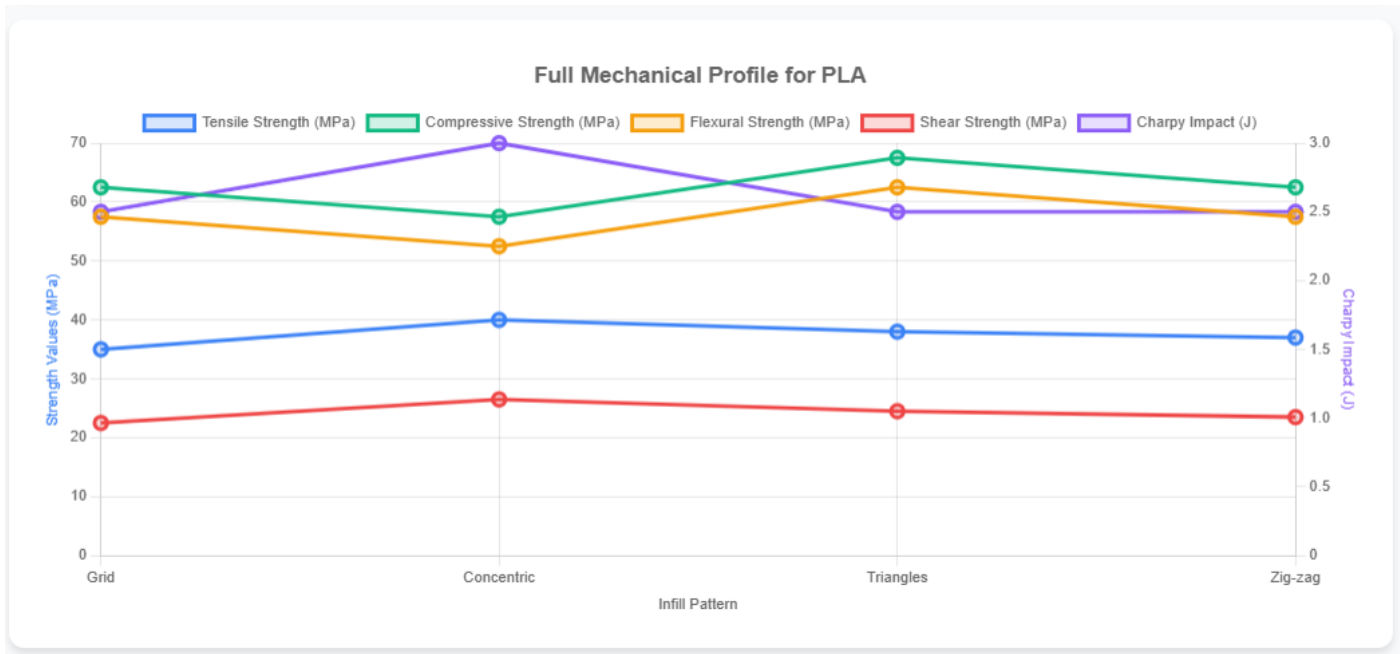


Fig 12.7: Line graph for overall view of the obtain values and the performance of the different patterns for different tests

4.2 ANALYSIS OF KEY PERFORMANCE MAXIMA

The experimental findings clearly indicate that no single infill pattern is optimal for all mechanical properties; a trade-off exists based on the required application:

- **Highest Tensile and Shear Strength (Concentric):** The Concentric pattern demonstrated the highest Tensile Strength (40 MPa) and Shear Strength (26.5 MPa). This geometry, which runs parallel to the perimeter, provides a continuous, strong load path, making it superior for resisting both pulling and layered-sliding forces.
- **Highest Compressive and Flexural Strength (Triangles):** The Triangles pattern achieved the maximum Compressive Strength (67.5 MPa) and Flexural Strength (62.5 MPa). Its rigid, interlocking truss structure efficiently distributes and resists internal stress under crushing and bending loads.
- **Highest Impact Resistance (Concentric):** The Concentric pattern was the toughest, absorbing the greatest amount of energy before fracture with a Charpy Impact Value of 3 J. The other three patterns (Grid, Triangles, and Zig-zag) all yielded a lower, identical value of 2.5 J.

5.CONCLUSION

This study examined how the mechanical performance of Polylactic Acid (PLA) specimens made using Fused Deposition Modeling (FDM) at a constant infill density of 60% was affected by various internal infill patterns,

including grid, triangle, concentric, and zigzag. Tensile strength, compressive strength, impact resistance, shear strength, and flexural strength were among the mechanical attributes evaluated.

The findings showed that the performance and structural integrity of PLA 3D printed objects are greatly impacted by the infill pattern selection. For applications where tensile and flexural strength are crucial, the concentric infill pattern continuously delivered superior results. The zigzag pattern, on the other hand, demonstrated exceptional impact resistance, suggesting that it is appropriate for components that are subjected to dynamic or impact pressures.

Although the grid design performed poorly in other mechanical tests, it demonstrated the maximum compressive strength, indicating that it is more appropriate for load-bearing applications where compressive stresses predominate. The best shear strength was provided by the triangular infill, demonstrating its benefit in situations with multidirectional loads.

Overall, the study emphasizes how crucial it is to modify infill designs according to particular mechanical specifications in order to maximize PLA parts' performance during additive manufacturing. Without changing the base material, engineers and manufacturers can improve the usefulness, strength, and longevity of 3D printed parts by choosing the right infill pattern.

To further increase the design options in FDM printing, future research might examine the combined impacts of infill density and printing parameters on hybrid materials or look at more intricate infill geometries.

6. REFERENCES

- Algarni, M., & Ghazali, S. (2021). Comparative study of the sensitivity of PLA, ABS, PEEK, and PETG's mechanical properties to FDM printing process parameters. *Crystals*, 11(8), 995.
- Alagheband, M., Zhang, Q., & Jung, S. (2024). Investigating the influence of infill patterns and mesh modifiers on fatigue properties of 3D printed polymers. *International Journal of Fatigue*, 187, 108463.
- Popa, C. F., Mărghițaș, M. P., Galațanu, S. V., & Marșavina, L. (2022). Influence of thickness on the IZOD impact strength of FDM printed specimens from PLA and PETG. *Procedia Structural Integrity*, 41, 557-563.

- Popa, C. F., Krausz, T., Galatanu, S. V., Linul, E., & Marsavina, L. (2023). Numerical and experimental study for FDM printed specimens from PLA under IZOD impact tests. *Materials Today: Proceedings*, 78, 326-330.
- Haque, M. M. M., Dhrubo, S. R., Pranto, A. F. Z., Ahmed, A., Arefin, M. M., Arifuzzaman, M., & Islam, M. S. (2025). Impact of Process Parameters and Material Selection on the Mechanical Performance of FDM 3D-Printed Components. *Hybrid Advances*, 100502.
- Mishra, A., & Jatti, V. S. (2023). Graph Neural Networks (GNN) for Tensile Strength Prediction in Additive Manufacturing.
- Hikmat, M., Rostam, S., & Ahmed, Y. M. (2021). Investigation of tensile property-based Taguchi method of PLA parts fabricated by FDM 3D printing technology. *Results in Engineering*, 11, 100264.
- Naveed, N., & Anwar, M. N. (2024). Optimising 3D printing parameters through experimental techniques and ANOVA-Based statistical analysis. *SPE Polymers*, 5(2), 228-240.
- Shanmugam, V., Babu, K., Kannan, G., Mensah, R. A., Samantaray, S. K., & Das, O. (2024). The thermal properties of FDM printed polymeric materials: A review. *Polymer degradation and stability*, 228, 110902.
- Ali, S. J., Rahmatabadi, D., Baghani, M., & Baniassadi, M. (2024). Experimental Evaluation of Mechanical Properties, Thermal Analysis, Morphology, Printability, and Shape Memory Performance of the Novel 3D Printed PETG-EVA Blends. *Macromolecular Materials and Engineering*, 309(10), 2400069.
- Patel, K. S., Shah, D. B., Joshi, S. J., Aldawood, F. K., & Kchaou, M. (2024). Effect of process parameters on the mechanical performance of FDM printed carbon fiber reinforced PETG. *Journal of Materials Research and Technology*, 30, 8006-8018.
- Ray, N. C., Saha, R. K., Mollah, M. E., Rakib, S., & Ali, Y. (2025). Enhancing Mechanical and Surface Properties of 3D-Printed Kevlar-Reinforced ABS/PLA Composites through FDM Process. *Hybrid Advances*, 100510.
- Pepeliaev, A., Lobov, E., Vindokurov, I., & Tashkinov, M. (2024). Comparison of mechanical properties of 3D-printed ABS, PA12 and PET-G reinforced with short fiber. *Procedia Structural Integrity*, 61, 224-231.